Interactions of Intercalative and Minor Groove Binding Ligands with Triplex Poly(dA)·[Poly(dT)]$_2$ and with Duplex Poly(dA)·Poly(dT) and Poly[d(A-T)]$_2$ Studied by CD, LD, and Normal Absorption†

Hye-Kyung Kim,‡ Jong-Moon Kim,‡ Seog K. Kim,*,‡ Alison Rodger,§ and Bengt Nordén||

Department of Chemistry, College of Sciences, Yeungnam University, Kyoungsan City, Kyoung-buk 712-749, Republic of Korea, Department of Chemistry, University of Warwick, Coventry CV4 7AL, England, and Department of Physical Chemistry, Chalmers University of Technology, S 412 96 Gothenburg, Sweden

Received August 14, 1995; Revised Manuscript Received November 3, 1995⊗

ABSTRACT: The binding of 9-aminoacridine and one bis-acridine compound to double helical poly(dA)·poly(dT) and poly[d(A-T)]$_2$ and triple helical poly(dA)·[poly(dT)]$_2$ has been investigated using linear dichroism (LD) and circular dichroism (CD). A close examination of the negative reduced LD and the induced CD for the first $\pi \rightarrow \pi^*$ transition absorption region leads us to conclude that the acridine moiety of the 9-aminoacridine and bis-acridine molecule intercalates with both duplex and triplex DNA. Binding geometries of the acridine moieties in the examined polynucleotides are similar to those found for the ligands with DNA (Hansen et al. (1984) *J. Chem. Soc., Chem. Commun.*, 509−511). It is also found that both 9-aminoacridine and bis-acridine effectively enhance the thermal stability of the triplex DNA. The corresponding spectra for the complexes of the minor groove binders DAPI and Hoechst with poly(dA)·[poly(dT)]$_2$ were studied for comparison. They both show a positive LD and a mixing ratio dependent positive CD in the ligand absorption region, similar to those of their duplex complexes. This indicates that these ligands bind in the grooves of the triplex, probably to the one corresponding to the minor groove of the template duplex.

Oligonucleotides that recognize double-stranded DNA *via* triple helix formation have drawn recent attention owing to the high selectivity of the third strand leading to the prospects of biological and therapeutic applications including the inhibition of transcription (Cooney et al., 1988; Postel et al., 1991; Young et al., 1991; Duval-Valentin et al., 1992; Grigoriev et al., 1992) or replication (Birg et al., 1990; Giovannangeli et al., 1993) of specific sequences, and the prevention of cellular proteins from binding to their designated target DNA (François et al., 1989; Maher et al., 1989; Hanvey et al., 1990). The formation of triple helices in which the third strand contains Fe(II)·EDTA or ellipticine derivatives has also been used to perform specific DNA cleavage (Strobel & Dervan, 1990, 1991; Perrouault et al., 1990). The importance of triple helices in biology is highlighted by the observation of intramolecular triplex (H-DNA) formation within supercoiled plasmids (Lyamichev et al., 1986; Htun & Dahlderg, 1988; Johnston, 1988).

In the formation of a triplex, thymines and protonated cytosines form Hoogsteen base pairs with, respectively, adenine and guanine bases of a duplex template. In general, the third Hoogsteen base-paired strand is less strongly bound to the duplex than are the two Watson−Crick bound strands of the corresponding duplex. In order to enhance the binding of the third strand under physiological condition, several approaches have been taken. The methods include use of photoactivated cross linking reagents (Takasugi et al., 1991; Giovannangeli et al., 1992), attaching intercalators to the third strand oligonucleotides (Sun et al., 1989), and use of triplex selective ligands such as benzopyridoindoles (BePI) which preferentially stablize the triplex structure (Mergny et al., 1992; Pilch et al., 1993a,b), all suggesting the importance of the ligand−DNA interaction. However, the number of studies of interactions between classical DNA binding drugs and triple helical polynucleotides are relatively few. Ethidium bromide (Scaria & Shafer, 1991; Tuite & Nordén, 1995) and BePI and its derivatives have been reported (Mergny et al., 1992; Pilch et al., 1993a,b) to intercalate between the base triplets, thereby stabilizing the third strand. Interactions between minor groove binding ligands and triple helical DNA have also been reported. NMR (Umemoto et al., 1990) and IR (Howard et al., 1992) have been used to show that distamycin binds to the triplex poly(dA)·[poly(dT)]$_2$. Since distamycin is known to bind highly selectively to the minor groove of B-form DNA, but not to A-form DNA (Zimmer & Wahnert, 1986), the fact that it binds to poly(dA)·[poly(dT)]$_2$ triplex suggests the triplex does indeed adopt a B-form conformation in solution. The binding of netropsin and berenil to the intramolecular triplex (dA)$_{12}$-x-(dT)$_{12}$-x-(dT)$_{12}$ (where x is a hexaethylene glycol chain) has been studied by CD and thermal denaturation (Durand et al., 1992, 1994), leading to the conclusions that the duplex- and triplex-bound ligands exhibit a similar conformation with netropsin destabilizing the third strand but berenil either stabilizing (when no NaCl is present) or destabilizing (when 1 M NaCl is present) the third strand.

† This work was supported in part by the Korea Science and Engineering Foundation (Grant 941-0300-020-2 defrayed to S.K.K.) and in part by the Basic Research Institute Program, Ministry of Education, Korea (Grant BSRI-94-3436 defrayed to S.K.K.). A.R. acknowledges the receipt of a travel award from the Royal Society.

* To whom correspondence should be addressed. Tel: 82 53 810 2362; Fax: 82 53 815 5412; e-mail: skkim@ynucc.yeungnam.ac.kr.

‡ Yeungnam University.

§ University of Warwick.

|| Chalmers University of Technology.

⊗ Abstract published in *Advance ACS Abstracts,* January 1, 1996.

0006-2960/96/0435-1187$12.00/0 © 1996 American Chemical Society

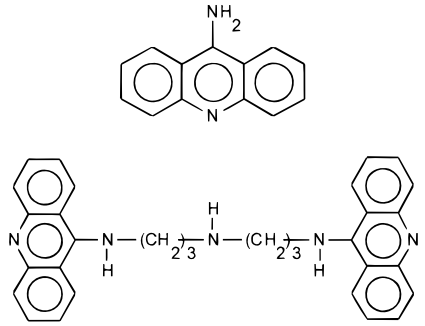

FIGURE 1: Molecular structure of 9AA and bis-9AA.

So far the binding geometries of the complexes formed between ligand and poly(dA)·[poly(dT)]$_2$ triplex have not been reported and no reason has been given for the different triplex stabilities induced by the ligands. The aim of the work reported in this paper was to probe how the interaction of different types of ligands with triplex DNA differed from that with related duplexes. We were particularly interested in the orientation of the ligands on DNA and in how the ligands affected DNA stability. As intercalators we used 9-aminoacridine (9AA) and bis-9-aminoacridine (bis-9AA), illustrated in Figure 1, which are two of the many acridine derivatives whose DNA binding has been studied (Hansen et al., 1984; Wirth et al., 1988). We have also included two known duplex minor groove binders in our study: 4′,6-diamidino-2-phenylindole (DAPI) and Hoechst 33258 (Hoechst). In this work, we report the LD and CD spectra of the triplex DNA/acridine derivatives and triplex DNA/minor groove binding ligand complexes and also the effect on the triplex DNA melting temperatures when ligands bind. The geometric implications of the results are discussed.

EXPERIMENTAL PROCEDURES

Materials

Polynucleotides, purchased from Pharmacia, were dissolved in 5 mM cacodylate buffer at pH 7.0, containing 20 mM NaCl and 1 mM EDTA, and dialyzed several times against 5 mM cacodylate buffer at pH 7.0. The poly(dA)·[poly(dT)]$_2$ triplex was prepared by incubating a 1:2 molar ratio of poly(dA) and poly(dT) at 90 °C for 30 min followed by overnight annealing at room temperature in 5 mM cacodylate buffer containing either 100 μM or 2 mM $MgCl_2$. Triplex formation was confirmed from its characteristic CD spectrum and melting profile. All measurements for poly(dA)·poly(dT) and poly[d(A-T)]$_2$ and their complexes were performed in 5 mM cacodylate buffer, and those for the poly(dA)·[poly(dT)]$_2$ triplex and its complexes were performed in the same buffer containing either 2 mM (for the spectroscopic study) or 100 μM $MgCl_2$ (for the melting curves). The concentrations of polynucleotides were determined spectrophotometrically using molar extinction coefficients: $\epsilon_{257nm} = 8600\ M^{-1}\ cm^{-1}$, $\epsilon_{264nm} = 8520\ M^{-1}\ cm^{-1}$, $\epsilon_{262nm} = 6600\ M^{-1}\ cm^{-1}$, and $\epsilon_{260nm} = 6000\ M^{-1}\ cm^{-1}$, respectively, for poly(dA), poly(dT), poly[d(A-T)]$_2$, and poly(dA)·poly(dT).

Bis-9AA was a gift from Professor Ole Buchardt of Copenhagen University. The minor groove binding drugs DAPI and Hoechst were purchased from Sigma and used without further purification. The concentrations of the ligands were determined spectrophotometrically using the molar extinction coefficients: $\epsilon_{400nm} = 9300\ M^{-1}\ cm^{-1}$ for 9AA, $\epsilon_{406nm} = 18\,000\ M^{-1}\ cm^{-1}$ for bis-9AA, $\epsilon_{340nm} = 27\,000\ M^{-1}\ cm^{-1}$ for DAPI, and $\epsilon_{338nm} = 42\,000\ M^{-1}\ cm^{-1}$ for Hoechst.

All spectroscopic measurements were performed for ligand−polynucleotide complexes of mixing ratios, *R*, of [ligand] per [base pair] or per [base triplet] of 0.02 and 0.25 for 9AA; 0.01 and 0.125 for bis-9AA; 0.039 and 0.190 for DAPI, 0.042 and 0.203 for Hoechst. In the bis-9AA case, each molecule possesses two ligands; therefore, half of the molar concentration compared to 9AA was used. The DNA concentration was usually 50 μM in base pair or base triplet for the spectroscopic studies and 25 μM for the melting curves. Resulting spectroscopic properties for the samples of above two ratios were usually essentially the same, indicating the binding properties are independent of the mixing ratio. For the case of bis-9AA binding to poly[d(A-T)]$_2$ a titration experiment with DNA concentrations ranging from 500 μM down to 40 μM was also performed for reasons discussed below. The results shown in this work are those for the higher mixing ratio in each case.

Methods

Normal Absorption. Absorption spectra were all run on a Cary 2300 spectrophotometer. All triplex spectra (except the melting curves) were measured in 2 mM $MgCl_2$ to ensure the triple helical conformation of the polynucleotide.

Melting Profiles. The dissociation of a polynucleotide strand from a double or triple helical polynucleotide manifests itself by hyperchromism in the absorbance in the 260 nm region. The polynucleotide "melting" point depends on various factors including the nature and concentration of the ions in solution. The melting profiles were measured on a HP 8452A diode array spectrophotometer equipped with a HP 80890A peltier temperature controller. The temperature was increased at a rate of 0.1 °C/min from 30 to 75−95 °C, with a reading being taken every 2 (acridines) or 3 (other ligands) min. The derivative spectra, dA/dT, were then calculated. The concentration of the triplex for the melting profile measurements was 25 μM in base triplet and 100 μM in $MgCl_2$.

CD. CD is defined to be the difference between the absorbance measured with left- and right-hand circularly polarized light. The CD spectra of the ligand−polynucleotide adducts can provide information on two levels. First, the conformation of polynucleotide itself can be probed through the CD of the intrinsic polynucleotide absorption near 260 nm. Second, although the drugs are all achiral molecules, they acquire an induced CD signal when they form complexes with a polynucleotide. The CD is induced by the interaction between the bound ligand and chirally arranged base transitions and is dependent upon the position and orientation with respect to the polynucleotide bases (Lyng et al., 1991,1992; Nordén et al., 1992). In some instances it is possible to extract this information. All CD spectra were measured on a Jasco J-720 spectropolarimeter (displaying the CD in millidegrees ellipcity) and were normalized with respect to concentration (M = mol·L^{-1}) and path length (cm).

LD and LD^r. LD is defined to be the differential absorption of the light polarized parallel ($A_{||}$) and perpen-

dicular ($A_\perp$) to some laboratory reference axis; in the case of flow LD, the || direction is the flow direction (Nordén et al., 1992). The measured LD spectrum is then divided by the isotropic absorption spectrum to give the reduced linear dichroism spectrum (LD^r):

$$LD^r(\lambda) = \frac{LD(\lambda)}{A_{iso}(\lambda)} \quad (1)$$

where A_{iso} denotes the isotropic absorption spectrum. The magnitude of an LD^r spectrum depends on two factors, namely, *S* and *O*, the orientation and optical factors, respectively (Nordén & Seth, 1985; Nordén et al., 1992; Nordén & Kurucsev, 1994).

$$LD^r(\lambda) = S \times O = 3S\frac{(\langle 3\cos^2\alpha\rangle - 1)}{2} \quad (2)$$

The optical factor depends on the angle, α, that the transition moment of the ligand makes with the polynucleotide helix axis. The brackets denote an ensemble average over the angular distribution (Nordén et al., 1992). The DNA bases have values close to 90°. Large values (80−90°) for ligands are indicative of intercalation, whereas values ranging from 40° to 50° are consistent with the transition lying along the minor groove. The orientation factor, *S*, reflects the degree of the orientation of polynucleotide in the flow; *S* would be unity for a polynucleotide perfectly aligned parallel to the flow direction and $S = 0$ for an isotropic sample. Assuming no overlap of DNA and ligand transitions, *S* may be determined from the polynucleotide dichroism at 260 nm, assuming an effective angle of 86° between the $\pi \rightarrow \pi^*$ transition moments of the nucleotide bases and the polynucleotide helix axis (Nordén et al., 1992). *S* depends on the contour length and flexibility of DNA, the flow rate, and the viscosity and temperature of the medium. The LD spectra of the oriented sample were measured by a Jasco J-500A spectropolarimeter equipped with an Oxley prism to convert the circularly polarized light from the CD spectropolarimeter into linearly polarized light as described elsewhere (Nordén & Seth, 1985). The orientation of the polynucleotide complexes was achieved using a flow Couette cell with outer rotating cylinder. The path length of the light of the Couette cell is 1 mm.

RESULTS

Absorption Spectroscopy. The binding of certain ligands to DNA produces hypochromism, broadening of the envelope, and a red shift of the ligand absorption bands. These effects are particularly pronounced for intercalators; with groove binders a large wavelength shift usually correlates with a ligand conformational change on binding or ligand−ligand interactions. The absorption spectra of the free ligands and the ligand absorption in the presence of the polynucleotide complexes (the absorption spectrum of the appropriate polynucleotide is subtracted for ease of comparison) are depicted in Figure 2. It should be noted that these spectra may have some free ligand contribution since the binding constants for these systems are estimated as low as 10^5 M^{-1}. This is discussed further below.

All the acridine−DNA complexes show 40−50% hypochromism at all wavelengths except for the poly(dA)·[poly(dT)]$_2$-9AA complex, which shows ∼30% hypochromism.

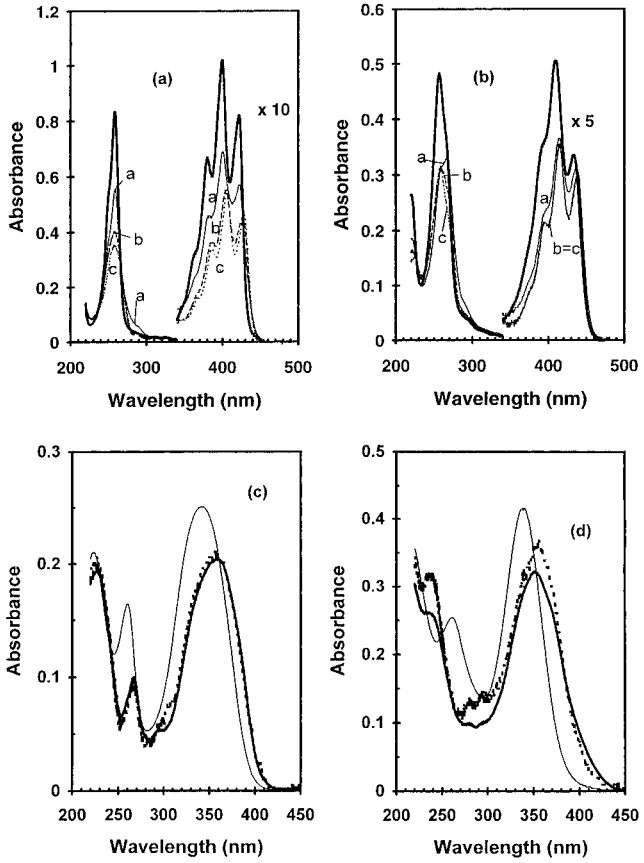

FIGURE 2: (a) and (b): Absorption spectra of 9AA (a) and bis-9AA (b) complexed with triple helical poly(dA)·[poly(dT)]$_2$ (curve a), double helical poly(dA)·poly(dT) (curve b), and poly[d(A-T)]$_2$ (curve c), and polynucleotide-free ligand (thick, solid curve). [Ligand] = 10 μM, [polynucleotide] = 50 μM in adenine base. (c) and (d): Absorption spectra of DAPI (1.94 μM (dotted curve) and 9.50 μM (solid curve)) and Hoechst (2.1 μM (dotted curve) and 10.50 μM (solid curve)), respectively, complexed with poly(dA)·[poly(dT)]$_2$ triplex. Absorbances are normalized to high ligand concentrations. Absorption spectra of corresponding polynucleotide are subtracted. That of polynucleotide-free ligand of high concentrations is denoted as a thin curve. [Polynucleotide] = 50 μM in adenine base.

The 259 nm (9AA) and 257 nm (bis-9AA) absorption peaks of the free ligands remain unshifted in all three complexes, but at longer wavelengths, a red shift of ∼4−6 nm is observed. The relative hypochromicity of the 257 nm maximum and the 267 nm shoulder for the poly(dA)·[poly(dT)]$_2$−bis-9AA complex results in a different spectral envelope for the bis-9AA triplex complex. Both triplex complexes show a small hyperchromism in normal absorption intensity in the 280−300 nm region compared to the corresponding duplex complexes.

The minor groove binding ligands also exhibit hypochromism and red shifts upon binding to the triplex that resemble their behavior with duplexes. The Hoechst spectral changes are slightly *R* dependent; at low mixing ratio ($R = 0.039$), 14% hypochromism and 16 nm red shift are observed, and as the mixing ratio was increased, the absorbance of the bound Hoechst decreased further and the peak shifts a little to *shorter* wavelength.

Melting Profiles. Figure 3 and Table 1 show the effect of the ligands on the thermal stability of poly[d(A-T)]$_2$, poly(dA)·poly(dT), and poly(dA)·[poly(dT)]$_2$ triplex. The melting profile of the duplexes occurs in a single step whereas that of the poly(dA)·[poly(dT)]$_2$ triplex is biphasic. The first

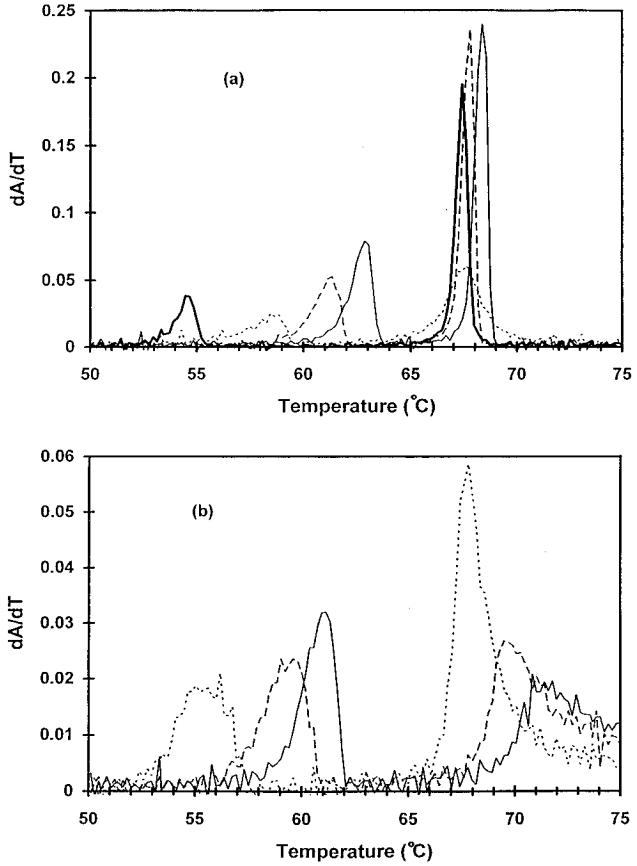

FIGURE 3: Thermal melting profiles of the poly(dA)·[poly(dT)]$_2$ triplex in the presence and absence of 9AA (a) and bis-9AA (b). Those for [ligand]/[base triplet] ratios of 0.1, 0.2, and 0.3 are marked as dotted, dashed, and solid curves, respectively. Melting profile of ligand-free triplex appears as a thick solid curve in (a). *A*(65 °C)/*A*(25 °C) is 1.14, 1.14−1.18, and 1.14, respectively, for ligand-free triplex, 9AA complex, and bis-acridine complex. *A*(75 °C)/*A*(25 °C) is 1.50 for triplex, 1.44 for the 9AA complex, and 1.31−1.44 for bis-acridine complex. In the bis-9AA complex case, the melting is not completed at 75 °C. The absorbance of the triplex is monitored at 260 nm in 5 mM cacodylate buffer containing 100 μM $MgCl_2$. The absorbance is recorded between 30 and 80 °C. [Polynucleotide] = 25 μM in base triplet.

Table 1: Melting Temperature of the Poly(dA)·[Poly(dT)]$_2$ Triplex in the Presence of Minor Groove Binders

	T_{m1} (°C)	T_{m2} (°C)
T:A:T	54.5	67.4
T:A:T + DAPI	42	94
T:A:T + Hoechst	41	89

[a] Ligand to base triplet ratio is 0.2.

melting temperature (T_m) of the triplex corresponds to the breaking of the Hoogsteen base pairing and the transition from poly(dA)·[poly(dT)]$_2$ to poly(dA)·poly(dT) plus poly(dT); it occurs at 54.5 °C under these salt conditions in the absence of any ligand. The second melting which corresponds to the dissociation of Watson−Crick base pairs, *i.e.*, the transition from the poly(dA)·poly(dT) duplex to poly(dT) plus poly(dA), occurs at 67.4 °C. Dissociation of the nonalternating duplex poly(dA)·poly(dT) occurs at 64.5 °C (data not shown) under the same salt conditions, thus confirming that the second transition is indeed the Watson−Crick one.

In presence of both 9AA and bis-9AA, the T_m for the third strand dissociation increases (Figure 3). As the mixing ratio

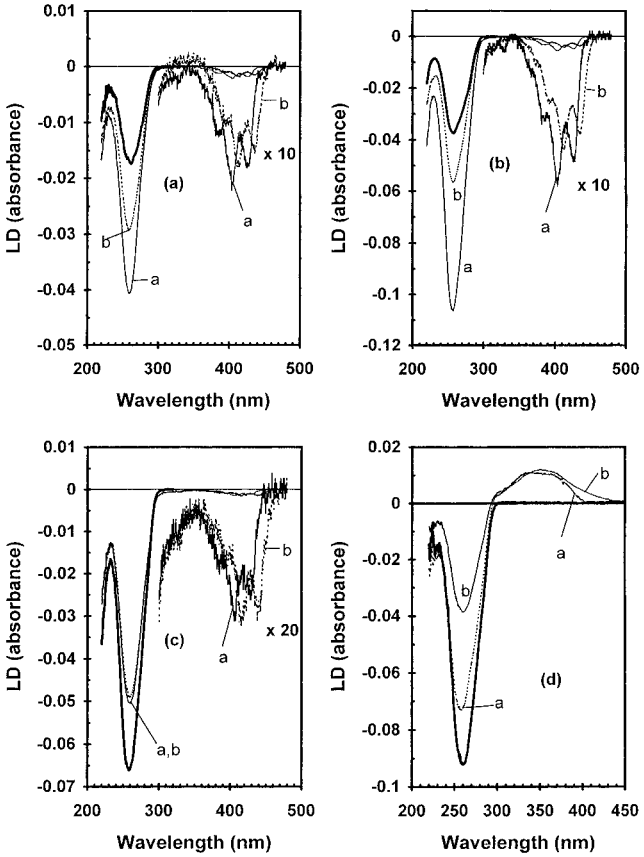

FIGURE 4: (a), (b), and (c): LD spectra of 9AA (curves a) and bis-9AA (curves b) complexed with poly[d(A-T)]$_2$ (a), poly(dA)·poly(dT) (b), and poly(dA)·[poly(dT)]$_2$ (c). The concentrations are the same as Figure 2. LD of corresponding ligand-free polynucleotide are depicted as thick, solid curves. (d): LD spectra of DAPI (curve a) and Hoechst (curve b) complexed with poly(dA)·[poly(dT)]$_2$ triplex. [DAPI] = 9.50 μM and [Hoechst] = 10.50 μM. [Polynucleotide] = 50 μM in adenine base. LD of ligand-free poly(dA)·[poly(dT)]$_2$ in the same conditions is shown as a thick solid curve.

increases from $R = 0.0$ to 0.1 to 0.2 to 0.3, the corresponding first T_m values are 54.5, 58.5, 61.3, and 62.8 °C for 9AA and 54.5, 55.6, 59.6, and 61.1 °C for bis-9AA. The values for the second T_m by way of contrast increase only from 67.4 to 68.4 °C with 9AA, and to 71.4 °C with bis-9AA. The profiles of the derivatives show much more dependence on ligand concentration, gradually becoming broader with bis-9AA. 9AA has a broad transition at $R = 0.1$, but the higher mixing ratios have profiles very similar to those of the free triplex.

The minor groove binders all affect the triplex stability differently from the acridines. They destabilize the binding of the third strand, resulting in T_m values of 41−42 °C for $R = 0.2$, compared with 54.5 °C for the free triplex. This result contrasts with the stabilization of the binding of the third strand of the oligo triplex when distamycin is present (Umemoto et al., 1990). The duplex is, however, significantly stabilized by each minor groove binder, resulting in a final T_m of about 90 °C.

LD and LD^r. The LD spectra of the acridine complexes are depicted in Figure 4a−c. DAPI and Hoechst complexed with triplex poly(dA)·[poly(dT)]$_2$ are shown in Figure 4 d. The two sets of spectra are extremely different. The acridine systems have a negative signal at all wavelengths, indicating that the transition moments are oriented on the average more

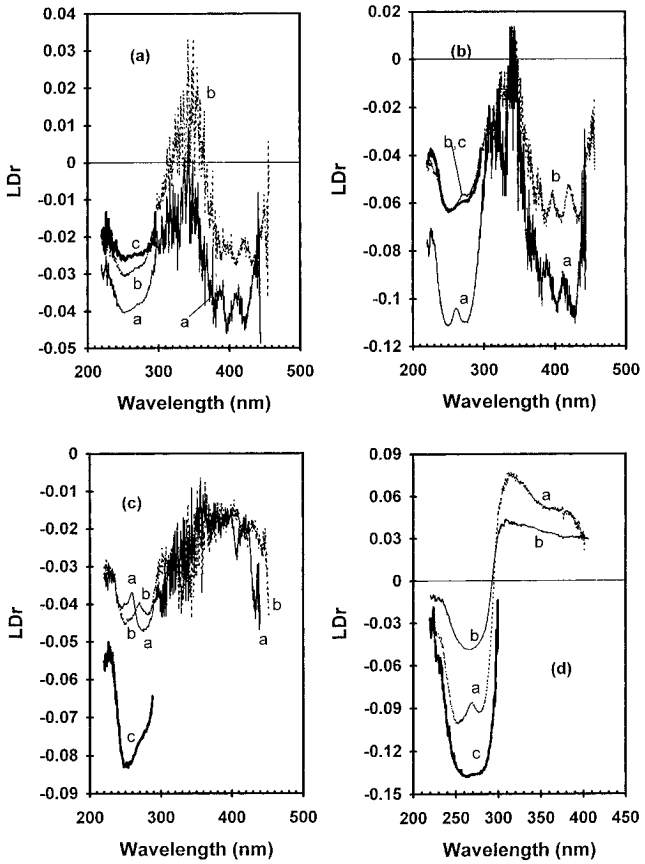

FIGURE 5: (a), (b), and (c): LD^r spectra of 9AA and bis-9AA complexed with poly[d(A-T)]$_2$ (a), poly(dA)·poly(dT) (b), and poly(dA)·[poly(dT)]$_2$ (c). (d): LD^r spectra the DAPI and Hoechst complexed with poly(dA)·[poly(dT)]$_2$ triplex. Curve assignments and conditions are the same as in Figure 4.

perpendicular than parallel to the helix axis. The spectra for the minor groove binding ligands are negative in the DNA region, in accordance with the DNA bases, which are perpendicular to the helix axis, dominating the spectrum, but in the ligand region the signal is positive. The LD^r spectra are determined from the LD by dividing by the absorption spectra of the bound ligands. The spectra of Figure 5 are adequate for all systems except the acridine−triplex complexes where either a lower binding constant or lower binding due to the ionic strength means that ∼40% of the 9AA and ∼30% of the bis-9AA (as determined from a simple dialysis experiment) are free. The LD^r spectra for the acridine−triplex complexes are therefore determined by first adjusting the normal absorption spectra of Figure 2. The qualitative interpretation of these spectra is unaffected by the percentages adopted.

The polarizations of the acridine transitions have been assigned from stretched film experiments (Matsuoka & Nordén, 1982; Fornasiero & Kuruscev, 1985): the 350-450 nm band is a single short axis polarized transition; the 340 nm region has a weak long axis polarized transition; at 280 nm weak transitions of both polarizations overlap; and at 260 nm there is an intense long axis polarized transition. Thus the LD^r spectra for the acridines at 400 nm indicate that the orientation of the short axis, at 260 nm, is dependent on both the DNA bases and the long axis of the ligands and, at 280 nm, is dominated by the DNA bases. The signal in the 340 nm region is not large enough to be analyzed.

The negative LD^r signal in the DNA region becomes very much stronger (*i.e.*, the DNA is more oriented) when 9AA binds to both duplexes (Figure 5a,b); with bis-9AA there is little change; the triplex complexes both show significant decrease in DNA orientation relative to the free triplex (Figure 5c), indicating the ligands have either increased the flexibility of the DNA, bent it, or contributed a positive LD signal of their own (both ligands absorb at 260 nm). The latter option may be ignored as the LD^r is reduced at both 260 and 280 nm.

The 350−450 nm ligand LD^r band for each acridine complex is in each case approximately the same magnitude as that of the DNA region, indicating that this short axis polarized transition lies parallel to the DNA bases in the bound complex. In contrast to previous LD studies on DNA−acridine systems, we have also found that the long axis of the acridines is parallel to the bases in all complexes since the LD^r at 260 nm is not smaller than that at 280 nm as was previously observed. In fact, the 260 nm LD^r in most of the complexes is noticeably larger relative to the free DNA than it is at 280 nm.

The LD^r for all minor groove binder complexes is negative for the polynucleotide in the $\pi \rightarrow \pi^*$ transition region around 260 nm, in accordance with the base planes of the DNAs being nearly perpendicular to the helix axis, and it is positive but not constant in the 340−400 nm region for all complexes. In this wavelength region, both DAPI and Hoechst are known to have more than one electronic transition moment of polarization within 10−20° of the long axis of the molecule (Kubista et al., 1989; Moon et al., 1995). The *S* values were taken from the LD^r at 260 nm of each spectrum and the angles were calculated from the LD^r values at 310 and 380 nm (using S value calculations from the 260 nm LD^r in each case). As the LD^r is not constant, we conclude the different transition moments do not have identical orientations with respect to the helix axis, but are approximately 45 ± 3° at both low and high *R* for the DAPI−triplex complex; 50 ± 1° (low *R*) and 40 ± 2° (high *R*) for the Hoechst−triplex complex (Figure 5d). These values are consistent with the ligands lying along a groove. The magnitude of LD^r in the DNA absorption region decreases for all complexes upon ligands binding to the triplex, suggesting that the ability of the triplex to orient along the flow lines is significantly impaired by the presence of ligands. This observation is in contrast to the increase in the LD^r for poly[d(A-T)]$_2$ when DAPI (Eriksson et al., 1993) or Hoechst binds to duplex (data not shown).

CD. The origin of the induced CD (ICD) signal for a ligand bound to a polynucleotide is quite complicated and extremely sensitive to the environment of the bound ligand (Lyng et al., 1991, 1992). Change in ICD in short wavelength (<300 nm) represents either a conformational change of the template DNA or an ICD of the bound ligand. Since the origin of the ICD in the short wavelength region is not clear, we shall restrict our discussion to longer wavelengths.

The ICD spectra (*i.e.*, the CD of the DNA plus ligand system with the CD spectrum of the corresponding polynucleotide subtracted) of the acridine ligands complexed with poly(dA)·poly(dT) and poly[d(A-T)]$_2$ duplexes and poly(dA)·[poly(dT)]$_2$ triplex, and of the minor groove binders with poly(dA)·[poly(dT)]$_2$ triplex, are shown in Figure 6. The 360−450 nm ICD spectra for 9AA with all three polynucleotides are similar (Figure 6a), showing small positive signals, with that due to the triplex being slightly

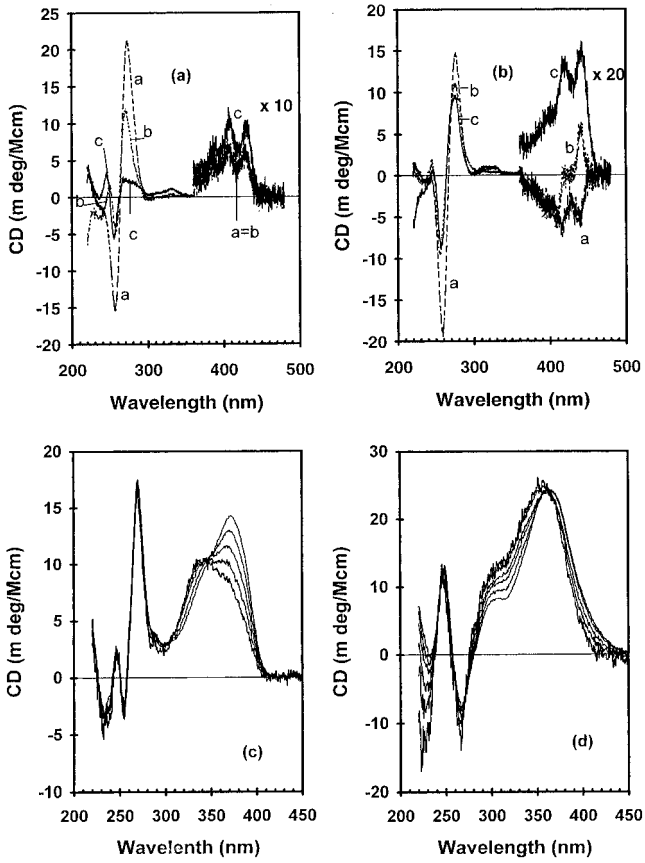

FIGURE 6: (a) and (b): Induced CD spectra of 9AA (a) and bis-9AA (b) complexed with double helical poly(dA)·poly(dT) (dotted curve b), poly[d(A-T)]$_2$ (curve a), and triple helical poly(dA)·[poly-(dT)]$_2$ (curve c). The concentrations are the same as in Figure 2. CD of corresponding polynucleotide was subtracted. (c) and (d): Induced CD spectra of DAPI (c) and Hoechst (d) complexed with triple helical poly(dA)·[poly(dT)]$_2$. [Triplex] = 50 μM in adenine base. [ligand/base triplet] = 0.077, 0.115, 0.153, 0.190, and 0.227 for the DAPI complex (from top to bottom at 380 nm) and 0.042, 0.083, 0.124, 0.164, 0.203, and 0.244 for Hoechst complex (from bottom to top at 330 nm). CD of corresponding polynucleotide was subtracted.

larger, despite its lower binding constant. These spectra are similar to those previously reported for this compound with calf thymus DNA (Fornasiero & Kuruscev, 1985). The sign of the 340 nm region ICD signal is also positive for 9AA, with the duplexes being larger for poly[d(A-T)]$_2$. Since the structure of this ICD band follows the vibrational spacing (Fornasiero & Kuruscev, 1985), we conclude that it is due mainly to a long axis polarized transition, not an n $\rightarrow \pi^*$ transition as previously suggested (Wirth et al., 1988). Relative to their normal absorption intensity, the duplex ICD signals in this region are large.

The ligand ICD spectra of the bis-9AA complexes in the 400 nm region differ significantly from those of the monomeric acridine 9AA. With the alternating duplex, the bis-9AA spectrum is approximately the negative of that observed for the monomer. The nonalternating duplex at $R = 0.1$ has a most unusual spectrum, being positive at longer wavelength and negative at shorter wavelength. A concentration titration (data not shown) shows that, at low R, the ICD is in fact the same as that with the alternating duplex. The most probable explanation of the high R spectral form is that we are observing the exciton coupling of the vibronic transitions. Figure 7 shows a sum of Gaussians that mimics such an

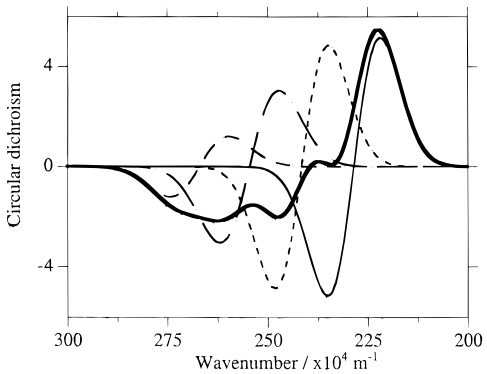

FIGURE 7: CD resulting from excition coupling of four vibronic bands. Component vibronic couplets are shown within these lines; net spectrum is the thick-line curve. The curve is resolved into a sum of Gaussians:

$$8.5\{\exp[-(x-225)^2/80] - \exp[-(x-232)^2/80]\} +$$
$$80\{\exp[-(x-238)^2/80] - \exp[-(x-245)^2/80]\} +$$
$$5.5\{\exp[-(x-251)^2/100] - \exp[-(x-258)^2/100]\} +$$
$$2.5\{\exp[-(x-264)^2/100] - \exp[-(x-270)^2/100]\}$$

excitonic coupling and produces the observed spectral form. In contrast to the duplex spectra, the ICD of the bis-9AA−poly(dA)·[poly(dT)]$_2$ complex is positive as is the monomer ICD. The ICD of bis-9AA in the 300−350 nm region is similar for the two duplexes and somewhat smaller for the triplex; all signals are positive.

The patterns of the acridine ICD spectra between 240 and 300 nm are similar, and the intensities are strong for all complexes. A negative minimum around 250−260 nm and a positive maximum at 270−280 nm is apparent. The spectral form is "excitonic" in appearance; however, the R dependence is small, which is not consistent with a large 9AA−9AA exciton interaction. Instead, we conclude this signal is due to exciton coupling with the DNA bases as has been previously observed for anthracene-9-carbonyl-N^1-spermine (Rodger et al., 1994) when the anthracene moiety intercalates. The positive CD in the 265−300 nm region of the 9AA−poly(dA)·[poly(dT)]$_2$ triplex complex is quite weak compared to that of the 9AA−duplex complexes.

The ICD spectrum of DAPI bound to poly[d(A-T)]$_2$ which at very low R has a positive feature with a maximum at 335 nm, at higher R shows a new and more intense induced CD band at 375 nm (Eriksson et al., 1993). Similar CD behavior is observed for the DAPI complexed with poly(dA)·[poly-(dT)]$_2$ (Figure 6c), though there is no evidence of the high R poly[d(A-T)]$_2$ spectrum that has a negative band at 425 nm. With the triplex, the ICD in the short wavelength (below 300 nm) is independent of R, but a significant mixing ratio dependence is observed in the wavelength longer than 300 nm. An isosbestic point at 345 nm suggests that there are two kinds of the bound DAPI. The CD spectrum at short wavelength (below 300 nm) could be due either to the change in the triplex conformation or to the induced CD of the bound DAPI or both.

The mixing ratio dependence of the induced CD spectrum of Hoechst (Figure 6d) bound to the poly(dA)·[poly(dT)]$_2$ triplex is similar to that of DAPI. Hoechst exhibits two types of CD in the long wavelength: at low R, the CD consists of a positive feature with a maximum around 355 nm and at higher R it has a maximum around 365 nm and an isosbestic point at 362 nm. This spectrum also resembles that observed when Hoechst binds to poly[d(A-T)]$_2$.

DISCUSSION

A number of conclusions follow from our comparative studies of a set of DNA binding ligands with the A-T rich duplexes: poly[d(A-T)]$_2$, poly(dA)·poly(dT), and the triplex poly(dA)·[poly(dT)]$_2$. The ligand set was chosen to include a simple intercalator (9AA), the related bis-intercalator with a minor groove binding linker (bis-9AA), and Hoechst and DAPI which are known to bind in the minor groove of A-T rich DNAs. The conclusions are as follows.

(1) The binding of each ligand to the triplex was found to be similar to its binding to the duplexes, with the acridines adopting modes parallel to the DNA bases and the groove binders being oriented along a groove.

(2) The binding strength of the acridine ligands to the triplex at the given mixing ratio is measured by equilibrium dialysis to be lower compared to the duplex (data not shown). The binding strength of DAPI and Hoechst was such that it was possible to assume all molecules were bound with each DNA.

(3) As evidenced by melting profiles, the triplex is stabilized relative to the duplex in the presence of the acridines with 9AA showing a greater effect (+8° at R = 0.2, versus +6.5° for bis-9AA), but the acridines had little (bis-9AA, +3° for R = 0.2) or very little (9AA, +1°) effect on the stability of the duplex. The minor groove binder, by way of contrast, caused the triplex to dissociate at a lower temperature (reduction of 13.5° and 12.5° in T_m at R = 0.2 respectively for DAPI and Hoechst), but stabilized the duplex (+21.6° to +26.6° for R = 0.2).

(4) All ligands caused a significant reduction in DNA orientation of the triplex in the flow LD experiment, whereas the simple intercalator significantly increased the degree of duplex orientation and the groove binders including bis-9AA had little effect.

(5) The effect of the bis-intercalator on the duplexes is an interesting combination of the effect of planar aromatic intercalators and a polyamine molecule. Polyamines such as spermidine bend DNA, and intercalators lengthen and stiffen DNA. As previously observed with anthracene-9-carbonyl-N^1-spermine (Rodger et al., 1994), the combination of these effects with the duplexes is too small an effect on DNA orientation to be noted.

(6) In contrast to previous LD studies of the acridine molecules bound to calf thymus DNA, we found (from the short axis polarized transitions at 400 and 280 nm and the long axis polarized ones at 265 and 280 nm) that both the short and long axes of the acridine moieties were approximately parallel to the DNA bases in all DNAs studied.

(7) The LD^r of the minor groove binder Hoechst with poly[d(A-T)]$_2$ is essentially flat across the three approximately long axis polarized transitions that occur in the ligand region of its spectrum. With the triplex, however, although the signal is consistent with the orientation of Hoechst on the triplex lying with its long axis along a groove, a wavelength dependence is observed, suggesting Hoechst is not oriented in exactly the same manner on both DNAs.

(8) The CD spectra of the acridines confirm that these molecules bind intercalatively. The absorption and LD^r spectra of the bis-9AA systems indicate both acridines are intercalated. At low R there is no ligand−ligand exciton interaction; however, at all R there is exciton coupling between some ligand transitions and the DNA transitions with which they are nearly degenerate. This effect is smallest with the 9AA−triplex complex.

(9) At intermediate values of R (0.1) bis-9AA bound to poly(dA)·poly(dT) shows significant ligand exciton coupling within the vibronic band of the 350−450 nm transition, resulting in the unusual spectral form oberved. Hoechst may also be showing some ligand−ligand interactions in both the poly[d(A-T)]$_2$ and the triplex complexes. No other acridine complexes give evidence of ligand−ligand interactions.

Although we cannot specify the binding geometries of these ligand−DNA complexes from our data, we can deduce some key features of the binding modes. First, consider how the acridines are oriented on the DNA. The LD and CD data lead us to conclude they are intercalated. The CD induced into the acridine transitions by the DNA is positive for all the 9AA ligand transitions outside the DNA region in all the complexes. For bis-9AA, the 350−450 nm (short axis polarized) band is negative for the duplexes, but the 340 nm long axis polarized transition is positive as in the other complexes. Such a sign change is often consistent with a rotation of the ligand by as much as 90° in the intercalation pocket. For poly[d(A-T)]$_2$, calculations (Lyng et al., 1992) would suggest that having the short axis along the intercalation pocket in a 5′T-3′A site is the most likely way to get a negative CD for an intercalator with this duplex. Transitions perpendicular to this or of either polarization in a 5′A-3′T site are predicted to have a positive CD signal. (In reality the ligand may well be angled in some way.)

The significant changes in DNA orientation upon complexation with the acridines give further information about the binding. 9AA increases the orientation of poly(dA)·poly(dT) yet reduces that of the poly(dA)·[poly(dT)]$_2$ triplex to less than the free duplex. Since the triplex is itself fairly inflexible, we conclude that when the acridine intercalates into the triplex, it bends it, presumably because it does not provide a driving force to hold the bases of the third strand apart also. Thus, it might be thought of as only partially intercalated. Bis-9AA reduces the triplex orientation by almost exactly the same amount as does 9AA, implying that only the acridines, not the linker, are responsible for bending the triplex (*cf.* with point (5) above).

The second general structural question we should address is what effect drugs have on the stabilization−destabilization mechanisms for the third strand of triplexes under physiological conditions. We have included two types of groove binders in this study: the planar aromatic minor groove binders and the polyamine linker of bis-9AA. All are known to prefer the minor groove of A-T rich DNAs, though the preference of polyamines for the major groove is not exclusive (Rodger et al., 1994).

There are three grooves in the triplex which could possibly be binding sites for the duplex minor groove binders. Those have been denoted the Watson−Crick (between strands I and II), Crick−Hoogsteen (between strands II and III), and Watson−Hoogsteen (between strands I and III) grooves (Radhakrishnan & Patel, 1994a−c). The Crick−Hoogsteen groove is narrow (2−3 Å) so that it may be excluded from consideration. The Watson−Hoogsteen groove is >7 Å wide and is somewhat hydrophobic due to the methyl group of thymine residues. The Watson−Crick groove (∼6−7 Å in width) corresponds to the minor groove of a B-form duplex. The spectroscopic characteristics of the minor groove binders bound to the triplex resemble those of the duplex, which

suggests the Watson−Crick groove is the favored binding site. In addition, there is a methyl group in the Watson−Hoogsteen groove which would hinder binding there, and Durand et al. have concluded that netropsin probably binds in the minor groove of $(dA)_{12}$-x-$(dT)_{12}$-x-$(dT)_{12}$ (Durand et al., 1992).

CONCLUSION

9AA and bis-9AA which are mono- and bis-intercalators with double helical B−DNA also intercalate in to poly(dA)·$[poly(dT)]_2$ triplex and stabilize the Hoogsteen paired third strand. The minor groove binders DAPI and Hoechst, by way of contrast, bind to one of the three grooves (probably the Watson−Crick groove) of the poly(dA)·$[poly(dT)]_2$ triplex and destablize the third strand.

REFERENCES

Birg, F., Praseuth, D., Zerial, A., Thuong, N. T., Asseline, U., Le Doan, T., & Hélène, C. (1990) *Nucleic Acids Res. 18*, 2901−2908.

Cooney, M., Czernuszewicz, G., Postel, E. H., Flint, S. J., & Hogan, M. E. (1988) *Science 241*, 456−459.

Durand, M., Thuong, N. T., & Maurizot, J. C. (1992) *J. Biol. Chem. 267*, 24394−24399.

Durand, M., Thuong, N. T., & Maurizot, J. C. (1994) *J. Biomol. Struct. Dyn. 11*, 1191−1202.

Duval-Valentin, G., Thuong, N. T., & Hélène, C. (1992) *Proc. Natl. Acad. Sci. U.S.A. 89*, 504−508.

Eriksson, S., Kim, S. K., Kubista, M., & Nordén, B. (1993) *Biochemistry 32*, 2987−2998

Fornasiero, D., & Kurucsev, T. (1985) *Chem. Phys. Lett. 117*, 176−180

François, J. C., Saison-Behmoaras, T., Thuong, N. T., & Hélène, C. (1989) *Biochemistry 28*, 9617−9619.

Giovannangeli, C., Thuong, N. T., & Hélène, C. (1992) *Nucleic Acids Res. 20*, 4275−4281

Giovannangeli, C., Thuong, N. T., & Hélène, C. (1993) *Proc. Natl. Acad. Sci. U.S.A. 90*, 10013−10017.

Grigoriev, M., Praseuth, D., Robin, P., Hemar, A., Saison-Behmoaras, T., Dautry-Varsat, A., Thuong, N. T., Hélène, C., & Harel-Bellan, A. (1992) *J. Biol. Chem. 267*, 3389−3395.

Hansen, J. B., Koch, T., Buchardt, O., Nielsen, P. E., Nordén, B., & Wirth, M. (1984) *J. Chem. Soc., Chem. Commun.*, 509−511.

Hanvey, J. C., Shimizu, M., & Wells, R. D. (1990) *Nucleic Acids Res. 18*, 157−161.

Howard, F. B., Todd Miles, H., Liu, K., Frazier, J., Raghunathan, G., & Sasisekharan, V. (1992) *Biochemistry 31*, 10671−10677.

Htun, H., & Dahlberg, J. E. (1988) *Sciences 241*, 1791−1796.

Johnston, B. H. (1988) *Science 241*, 1800−1804.

Kubista, M., Åkerman, B., & Albinsson, B. (1989) *J. Am. Chem. Soc. 111*, 7031−7035.

Lyamichev, V. I., Mirkin, S. M., & Frank-Kamenetskii, M. D. (1986) *J. Biomol. Struct. Dyn. 3*, 667−669.

Lyng, R., Rodger, A., & Nordén, B. (1991) *Biopolymer 31*, 1709−1720.

Lyng, R., Rodger, A., & Nordén, B. (1992) *Biopolymer 32*, 1201−1214.

Maher, L. J. III., Wold, B., & Dervan, P. B. (1989) *Science 245*, 725−730.

Matsuoka, Y., & Nordén, B. (1982) *Chem. Phys. Lett. 85*, 302−306.

Mergny, J. L., Duval-Valentin, G., Nguyen, C. H., Perrouault, L., Faucon, B., Rougée, M., Montenay-Garestier, T., Bisagni, E., & Hélène, C. (1992) *Science 256*, 1681−1684.

Moon, J.-H., Kim, S. K., Sehlstedt, U., Rodger, A., & Nordén, B. (1995) *Biopolymer* (in press).

Nordén, B., & Seth, S. (1985) *Appl. Spectrosc. 39*, 647−655.

Nordén, B., & Kurucsev, T. (1994) *J. Mol. Recognit. 7*, 141−156.

Nordén, B., Kubista, M., & Kurucsev, T. (1992) *Q. Rev. Biophys. 25*, 51−170.

Perrouault, L., Asseline, U., Rivalle, C., Thuong, N. T., Bisagni, E., Giovannangeli, C., Le Doan, T., & Hélène, C. (1990) *Nature 344*, 358−360.

Pilch, D. S., Martin, M.-T., Nguyen, C. H., Sun, J.-S., Bisagni, E., Garestier, T., & Hélène, C. (1993a) *J. Am. Chem. Soc. 115*, 9942−9951

Pilch, D. S., Waring, M. J., Sun, J.-S., Rougée, M., Nguyen, C. H., Garestier, T., & Hélène, C. (1993b) *J. Mol. Biol. 232*, 926−946.

Postel, E. H., Flint, S. J., Kessler, D. J., & Hogan, M. E. (1991) *Proc. Natl. Acad. Sci. U.S.A. 88*, 8227−8231.

Radhakrishnan, I., & Patel, D. J. (1994a) *Biochemistry 33*, 11405−11416.

Radhakrishnan, I., & Patel, D. J. (1994b) *Structure 2*, 395−405.

Radhakrishnan, I., & Patel, D. J. (1994c) *J. Mol. Biol. 241*, 600−619.

Rodger, A., Blagbrough, I. S., Adlam, G., & Carpenter, M. L. (1994) *Biopolymer 34*, 1583−1593

Scaria, P. V., & Shafer, R. H. (1991) *J. Biol. Chem. 266*, 5417−5423.

Strobel, S. A., & Dervan, P. B. (1990) *Science 249*, 73−75.

Strobel, S. A., & Dervan, P. B. (1991) *Nature 350*, 172−174.

Sun, J. S., François, J. C., Montenay-Garestier, T., Saison-Behmoaras, T., Roig, V., Thuong, N. T., & Hélène, C. (1989) *Proc. Natl. Acad. Sci. U.S.A. 86*, 9198−9202

Takasugi, M., Guendouz, A., Chassignol, M., Decout, J. L., Lhomme, J., Thuong, N. T., & Hélène, C. (1991) *Proc. Natl. Acad. Sci. U.S.A. 88*, 5602−5606

Tuite, E., & Nordén, B. (1995) *Bioorg. Med. Chem. 3*, 701−711.

Umemoto, K., Sarma, M. H., Gupta, G., Luo, J., & Sarma, R. H. (1990) *J. Am. Chem. Soc. 112*, 4539−4545.

Wirth, M., Buchardt, O., Koch, T., Nielsen, P. E., & Nordén, B. (1988) *J. Am. Chem. Soc. 110*, 932−939

Young, S. L., Krawczyk, S. H., Matteucci, M. D., & Toole, J. J. (1991) *Proc. Natl. Acad. Sci. U.S.A. 88*, 10023−10026.

Zimmer, Ch., & Wahnert, U. (1986) *Prog. Biophys. Mol. Biol. 41*, 31−112.

BI951913M